RSC Advances

REVIEW

View Article Online
View Journal | View Issue

Cite this: *RSC Adv.*, 2022, **12**, 16927

Applications of nanocomposites based on zeolitic imidazolate framework-8 in photodynamic and synergistic anti-tumor therapy

Wen Kang, [a] Ying Tian, [b] Ying Zhao, *[a] Xindao Yin *[a] and Zhaogang Teng *[c]

Due to the limitations resulting from hypoxia and the self-aggregation of photosensitizers, photodynamic therapy (PDT) has not been applied clinically to treat most types of solid tumors. Zeolitic imidazolate framework-8 (ZIF-8) is a common metal–organic framework that has ultra-high porosity, an adjustable structure, good biocompatibility, and pH-induced biodegradability. In this review, we summarize the applications of ZIF-8 and its derivatives in PDT. This review is divided into two parts. In the first part, we summarize progress in the application of ZIF-8 to enhance PDT and realize theranostics. We discuss the use of ZIF-8 to avoid the self-aggregation of photosensitizers, alleviate hypoxia, increase the PDT penetration depth, and combine PDT with multi-modal imaging. In the second part, we summarize how ZIF-8 can achieve synergistic PDT with other anti-tumor therapies, including chemotherapy, photothermal therapy, chemodynamic therapy, starvation therapy, protein therapy, gene therapy, and immunotherapy. Finally, we highlight the challenges that must be overcome for ZIF-8 to be widely applied in PDT. To the best of our knowledge, this is the first review of ZIF-8-based nanoplatforms for PDT.

Received 19th February 2022
Accepted 6th May 2022

DOI: 10.1039/d2ra01102f

rsc.li/rsc-advances

Introduction

Cancer is an urgent problem that threatens human life and health,[1] and how to cure cancer at the lowest possible cost is an important issue. Traditional cancer treatments such as surgery, chemotherapy, radiation therapy, and immunotherapy have several side effects.[2–4] The application of nanomaterials in the biomedical field provides a new direction for cancer researchers. Nanomaterials can be applied to facilitate

[a]*Department of Radiology, Nanjing First Hospital, Nanjing Medical University, Nanjing 210006, P. R. China. E-mail: zhaoyingmed@163.com; y.163yy@163.com; tzg@fudan.edu.cn*

[b]*Department of Radiology, Affiliated Hospital of Nanjing University of Chinese Medicine, Nanjing 210029, P. R. China*

[c]*Key Laboratory for Organic Electronics and Information Displays and Institute of Advanced Materials (IAM), Nanjing University of Posts and Telecommunications, Nanjing 210046, P. R. China*

Wen Kang, was born in Jiangsu, China, in 1997. She received her B. S. Med degree (2015) from Jiangsu University and is studying for a M. S. degree at Nanjing Medical University. Her current research focuses on the molecular imaging fields.

Ying Tian received her B. S. degree from Dezhou University in 2006, obtained her M. S. degree in biochemistry and molecular biology from Nanjing Normal University in 2009, respectively. She got a PhD degree in clinical medicine from Nanjing University in 2020. Since 2010, she has been working as an associate researcher at Jinling hospital. From 2021, she changed her unit to affiliated hospital of Nanjing University of Chinese Medicine, and further continued her research in diagnosis and treatment of tumor.

controlled drug transport, reduce side effects in normal tissues, and improve the curative effect of cancer treatment.[5,6] At present, liposomes, polymeric micelles, and inorganic nanoparticles [NPs; *e.g.*, gold NPs (AuNPs), magnetic NPs, upconversion NPs (UPNPs), and mesoporous silica NPs] are widely used in drug delivery systems.[7,8] However, the hypersensitivity of liposomes, immunogenicity and complicated biological characteristics of polymeric micelles, and the toxicity of inorganic NPs restrict their clinical applications.[9–12] In recent years, metal–organic frameworks (MOFs) have attracted considerable attention as a new type of nanomaterial. MOFs are a class of porous materials composed of metal ions or their clusters coordinated with organic ligands.[13] Conventional MOFs have various advantages, including ultra-high porosity, high surface area, and adjustable structure,[14–16] giving MOFs great potential in gas storage,[17] chemical separation,[18,19] catalysis,[20,21] sensing,[22] drug delivery,[23] and other fields. Nanoscale MOFs (nMOFs) display high drug loading efficiency, high biodegradability, and low biological toxicity.[24] Thus, nMOFs are regarded as ideal nanocarriers of biomacromolecules.[25]

Zeolitic imidazolate framework-8 (ZIF-8) is a common MOF constructed from zinc ions and 2-methylimidazole (H-MeIM). ZIF-8 was first synthesized by Park and colleagues in 2006 *via* a solvothermal method.[26] In this solvothermal synthesis, zinc nitrate tetrahydrate and H-MeIM were mixed and dissolved in dimethylformamide (DMF). After heating (5 °C min^{-1}) the solution to 140 °C and keeping this state for 24 h, the solution was cooled (0.4 °C min^{-1}) to room temperature. Then the mother liquor was removed, and chloroform was added. Colorless polyhedral crystals were collected from the upper layer, washed with DMF, and dried in air to obtain ZIF-8. In comparison to other MOFs, ZIF-8 has better biocompatibility because it is composed of constituents of the physiological system.[27,28] Under physiological conditions (pH 7.4) and alkaline conditions, ZIF-8 shows excellent chemical and thermal stability. However, acidic conditions (pH 5.0–6.0) destroy the coordination between H-MeIM and zinc ions, leading to the decomposition of the ZIF-8 structure.[26] This feature allows the construction of pH-controlled drug delivery systems based on ZIF-8.[29] Since the first solvothermal synthesis of ZIF-8, additional solvothermal methods along with microwave-assisted, sono-chemical, mechanochemical, dry-gel, microfluidic, and high-throughput methods have been reported to synthesize ZIF-8 (Fig. 1).[26,30–36] ZIF-8 NPs with different average particle sizes can be obtained using different synthetic methods. Among reported methods, the solvothermal synthesis of ZIF-8 in DMF results in the largest particle size (approximately 150–200 μm). ZIF-8 with relatively uniform particle sizes can be synthetized *via* sono-chemical routes.

The delivery of functional molecules by ZIF-8 is typically based on pore encapsulation, the core–shell structure, surface attachment, ion doping, and *in situ* growth (Fig. 2).[37–40] However, due to the small apertures (diameter of approximately 3.4 Å) of ZIF-8,[41] some drugs can only be adsorbed on the surface of ZIF-8. To solve this problem, Tsung and colleagues developed a general one-pot synthetic route to encapsulate small molecules and improve the drug-loading capacity of ZIF-8; they incorporated fluorescein to imitate drugs that are larger than the ZIF-8 apertures. Zinc nitrate hexahydrate (150 mg) and H-MeIM (330 mg) were dissolved in 7.15 mL of methanol. After fluorescein-containing methanol solution was mixed with the zinc solution, H-MeIM solution was added into the zinc-based solution under magnetic stirring for 5 min. The change in

Ying Zhao received her B. S. degree and PhD degree in Clinical Medicine from Nanjing University in 2015 and 2018, respectively. After her PhD she joined the Department of Radiology, Nanjing First Hospital, and worked on molecular imaging. Her research focuses on the nanomedicine, multimodality imaging and synergistic therapy of tumor.

Xindao Yin, received his B. S. (1989) and M. S. degree (1996) from Suzhou University. He obtained his PhD in Medical Imaging and Nuclear Medicine from Fudan University. Since 2009 he has become a chief physician. He is an associate professor at Nanjing Medical University. His research interests include molecular imaging, functional imaging and diagnostic imaging.

Zhaogang Teng received his B. S. (2004) and PhD (2009) from Jilin University. He conducted postdoctoral research at Fudan University from 2009 to 2011. Then he worked at Jinling Hospital from 2011 to 2019. He currently works at Department of Materials Science and Engineering of University of Posts and Telecommunications. He has published more than 100 peer reviewed papers. His research interests focus on the synthesis of porous nanoparticle, interfacial chemistry, and nanomedicine.

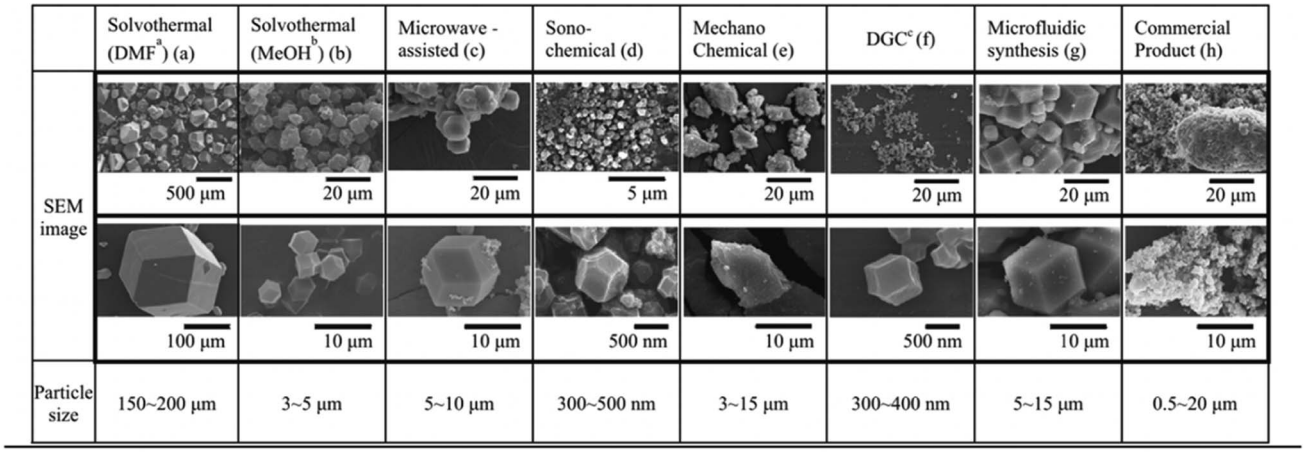

Fig. 1 SEM images and particle sizes of ZIF-8 samples prepared using different synthetic methods. [This figure has been reproduced from ref. 36 with permission from Elsevier Inc., copyright 2015].

color of the solution from bright green to milky white indicated the formation of ZIF-8 NPs. The obtained solution was centrifuged at 7000 rpm for 10 min and washed with methanol to obtain the fluorescein-loaded ZIF-8.[28] This general process provides an effective method to embed different therapeutic molecules in ZIF-8 and expands the available ZIF-8-based strategies for tumor treatment.

Generally speaking, photodynamic therapy (PDT) is a kind of phototherapy in which singlet oxygen ($^1O_2$) and reactive oxygen species (ROS) are produced to kill tumor cells at the areas of photosensitizer (PS) accumulation under light irradiation at a specific wavelength [generally ultraviolet, visible, or near-infrared (NIR) light] and dose.[42–44] PDT kills tumor cells directly or indirectly by inducing cell apoptosis, necrosis, and/or autophagy, triggering inflammation and immune response, and damaging the vasculature system.[45–47] For PDT to be effectively applied in cancer treatment, a combination of light, a PS, and O_2 is required. However, the hypoxia of tumor sites and the nonselective distribution of PSs limit the therapeutic efficacy of conventional PDT.[46] Because ZIF-8 can be used to load PSs,[48] it has great prospects in PDT for cancer. This review summarizes PDT-related nanocomposites based on ZIF-8 and its derivatives (Table 1) and discusses problems related to these nanoplatforms.

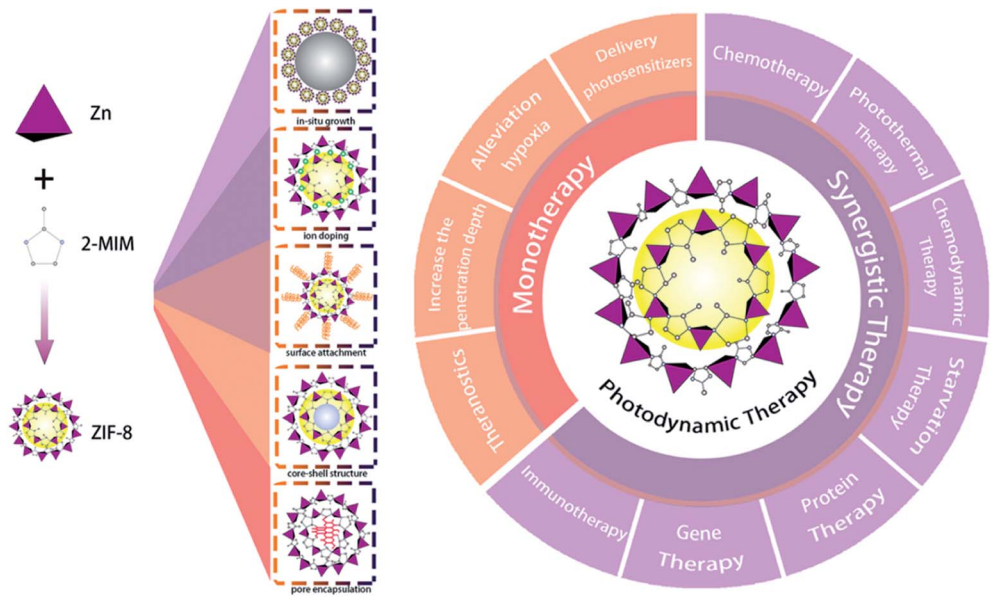

Fig. 2 Schematic overview of common strategies to deliver functional molecules and the applications of ZIF-8 nanoplatforms in photodynamic therapy and synergistic therapy.

Table 1 Summary of nanoplatforms based on ZIF-8 and its derivatives for monotherapy or synergistic PDT (* indicates a derivative-based nanoplatform)

Therapy modalities	Nanoplatforms	Payloads	Ref.
Monotherapy			
PS delivery	ZnPc@ZIF-8	ZnPc	53
	ZnPc–COOH@ZIF-8	ZnPc–COOH	54
	ZIF-8@Ce6-HA	Ce6	57
	$MPEG_{2000}$-ZIF/PC	PC	64
	PS@ZIF-8-PMMA-S-S-mPEG	D–A photosensitizers	68
Alleviation of hypoxia	CAT-PS-ZIF@Mem	$AlPcS_4$, CAT	75
	UCNPs/MB@ZIF-8@catalase	UCNPs, MB, CAT	78
	Au@ZIF-8	AuNPs, Ce6	84
Increase the penetration depth	UCNPs-g-C_3N_4–CDs@ZIF-8	g-C_3N_4, CDs, UCNPs	89
Multi-modal imaging-guided PDT	BSA–MnO_2/Ce6@ZIF-8	Ce6, (BSA)-MnO_2	94
	ZIF-8–IR820–MnPc–HA	IR820, MnPc	99
Synergistic PDT			
PDT and chemotherapy	g-C_3N_4@ZIF-8	g-C_3N_4, DOX	102
	AuNCs@MOF-DOX	AuNCs, DOX	103
	F127–MnO_2-ZIF@DOX/C_3N_4	g-C_3N_4, MnO_2, DOX	105
	ZDZP@PP	DOX, PpIX	106
	BCP/Cit-Fe(III)@ZIF-8	DOX, BCP, Cit-Fe(III)	108
	FZIF-8/DOX-PD-FA -	DOX, Ce6	112
PDT and PTT	Fe_3O_4/ZIF-8-Au_{25}	$Au_{25}(SR)_{18}^-$, Fe_3O_4	48
	PDAs-MB-CAT-ZIF-8	MB, CAT, PDAs	118
	ZCNs*		119
PDT and CDT	O_2–Cu/ZIF-8@Ce6/ZIF-8@F127	O_2, Cu^{2+}, Ce6	71
PDT and ST	UCNPs/TAPP@ZIF-8@Catalase/GOx	UCNPs, TAPP, CAT, GOx	73
	PEG-COOH@Enzymes@TPP–DNB@ZIF-8	TPP–DNB, CAT, GOx	130
PDT and protein therapy	Ce6/Cyt c@ZIF-8/HA	Cyt c, Ce6	134
PDT and gene therapy	DNAzyme@ZIF-8	DNAzyme	138
PDT, PTT, and chemotherapy	FeNC@PAA*		143
PDT, CDT, and ST	Ce6/GOx@ZIF-8/PDA@MnO_2	GOx, MnO_2, Ce6	146
PDT, CDT, and chemotherapy	MIL-88-ICG@ZIF-8-DOX	ICG, DOX	147
	(DOX and ICG)@H-PMOF@mem*	ICG, DOX	150
PDT, PTT, chemotherapy, and immunotherapy	CuZPMn@CpG	PpIX, CuS, DOX, CpG, MnO_2	151

Individual PDT nanoplatforms

PS delivery. PSs, which are one of the three crucial factors in PDT, largely determine the therapeutic efficiency of PDT. PSs are usually divided into different generations. First-generation PSs are complex natural mixtures and include hematoporphyrin derivatives.[49] Photofrin®, the first Food and Drug Administration-approved PS for clinical treatment, is excited by a 630 nm laser, leading to poor tissue penetration.[50,51] Second-generation PSs are pure synthetic compounds. Most second-generation PSs are based on porphyrin and chlorin structures that absorb in the region of 650–750 nm. Compared to first-generation PSs, second-generation PSs are irradiated by light with a longer wavelength (650–850 nm) and can penetrate more deeply into tissue.[52] Second-generation PSs usually have poor tumor selectivity, and most are hydrophobic, leading to self-aggregation in aqueous solution. As a result, the fluorescence is rapidly quenched, leading to a local reduction in ROS generation.[24] Moreover, the poor water solubility of second-generation PSs limits their application by intravenous administration. To increase the PS solubility and enhance PS specific accumulation in tumors, third-generation PSs have been developed by combining traditional second-generation PSs with drug delivery systems including liposomes, NPs, and monoclonal antibodies.[49] Because the therapeutic efficacy of third-generation PSs depend on actual PSs, the limitations of traditional PSs need to be overcome. For example, zinc(II) phthalocyanine (ZnPc) was enclosed in the micropores of ZIF-8 to form ZnPc@ZIF-8 *via* a one-step coprecipitation route to prevent the self-aggregation of ZnPc and fluorescence quenching in aqueous solution.[53] ZnPc@ZIF-8 shows good biodegradability because of its disassembly in the acidic tumor microenvironment (TME). Song *et al.* also developed a pH-responsive drug delivery system based on ZIF-8, termed ZnPc–COOH@ZIF-8.[54] ZnPc–COOH@ZIF-8 realized passive tumor targeting *via* the release of ZnPc in the acidic TME. Similarly, hydrophobic Chlorin e6 (Ce6) was encapsulated into ZIF-8 to prevent its self-aggregation *via* a one-pot process.[51,55–57] The surface of ZIF-8 was modified with hyaluronic acid (HA), a significant component of the extracellular matrix,[58] *via* covalent bonds, resulting in an active targeting effect. CD44 and CD44-like receptors are relatively over-expressed in many solid tumors.[59,60] CD44 can bind HA fragments *via* HA-binding domains in a region (amino acids 31–120 at the N-terminus) homologous to the B loop of cartilage link protein.[61,62] Compared with ZIF-8@Ce6, ZIF-8@Ce6-HA has

a longer blood circulation time and lower hepatotoxicity due to the presence of HA.

ZIF-8 has also been employed to encapsulate phycocyanin, an unstable new PS, *via* co-precipitation.[63,64] Together, the ZIF-8 skeleton and $MPEG_{2000}$–COOH modified on the surface of ZIF-8 greatly improved the stability and cell uptake of phycocyanin. At the same time, papaverine, an inhibitor of mitochondrial complex I,[65] combined with $MPEG_{2000}$-ZIF/phycocyanin to overcome hypoxia by restricting mitochondrial respiration at tumor sites and increasing ROS production for efficient PDT.

Another way to overcome PS inefficiency is to introduce donor (D) and acceptor (A) molecules to develop D–A PSs.[66,67] For example, Wang *et al.* utilized ZIF-8 to construct a nanocarrier (PS@ZIF-8-PMMA-S–S-mPEG) to handle the problem that water molecules reduce the efficiency of D–A PSs (Fig. 3).[68] The carrier realized the self-assembly of PS-loaded ZIF-8 *in vivo*. In this system, poly(methyl methacrylate) (PMMA) and disulfide-linked methoxy polyethylene glycol (S–S-mPEG) were connected with ZIF-8. The reduction of the disulfide bond and cleavage of mPEG led to the self-assembly of PS@ZIF-8-PMMA by PMMA fusion between adjacent nanoplatforms in tumor cells. These self-assemblies, which had sizes exceeding 200 nm, helped reduce drug extravasation and extend the retention time of organic PSs in tumors.[69] ZIF-8 can separate PSs from water and carry O_2 for PDT, thereby enhancing ROS generation in cancer PDT.

Alleviation of hypoxia. The TME is characterized by hypoxia, resulting in the low efficacy of PDT.[70] Existing strategies employed to alleviate hypoxia include the use of O_2 carriers, the adjustment of the TME, synergistic PDT, hypoxia-independent/dependent PDT and fractional PDT.[11] Researchers have directly loaded O_2, catalase (CAT), and CAT-like materials on nanoplatforms.[71–74] Cheng *et al.* co-embedded CAT as an O_2 generator and a second-generation photosensitizer [Al(III) phthalocyanine chloride tetrasulfonic acid ($AlPcS_4$)] in ZIF-8 to alleviate hypoxia. In other studies, the surface of a CAT-PS-ZIF-8 nanocomposite was covered with cancer cell membrane (Mem) to form CAT-PS-ZIF@Mem,[75] which delivered abundant Mem proteins and mimicked the antigenic diversity of the source cells to avoid an immune response and prolong blood circulation,[76,77] thereby improving the specific delivery of the PS. Cai *et al.* modified the surface of ZIF-8 with CAT to construct a highly productive NIR/hydrogen peroxide (H_2O_2)-responsive core–shell nanocomposite (termed UCNPs/MB@ZIF-8@catalase).[78] UCNPs ($NaYF_4$: 60% Yb/2% Er) and methylene blue (MB) were incorporated with ZIF-8 *via* a one-pot synthetic method. UCNPs are highly photostable for NIR imaging and emit anti-Stokes luminescence at wavelengths shorter than the absorption wavelength.[79–81] The combination of UCNPs and MB can guarantee fluorescence resonance energy transfer due to the spectral overlap between UCNP emission and MB absorption, which

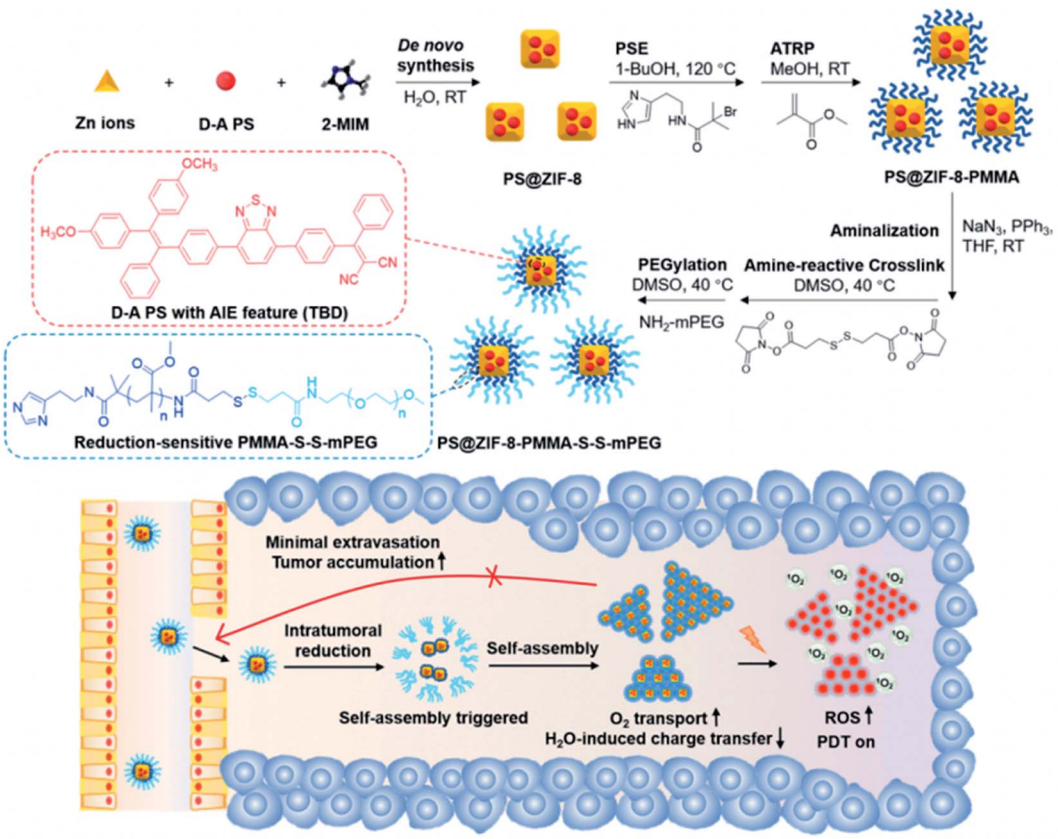

Fig. 3 Schematic of the self-assembly of PS@ZIF-8-PMMA-S–S-mPEG. [This figure has been reproduced from ref. 68 with permission from American Chemical Society, copyright 2020].

facilitates the production and release of $^1O_2$ and promotes efficient PDT.[82,83]

ZIF-8 was also used as a vehicle for CAT-like materials in an O_2 self-sufficient nanoplatform (Au@ZIF-8) in which AuNPs were connected to the surface of ZIF-8.[84] In addition to emitting fluorescence, AuNPs can simulate CAT-like properties.[85] Au@ZIF-8 can catalyze endogenous H_2O_2 to produce O_2 and relieve tumor hypoxia, thereby enhancing the curative effect of PDT. ZIF-8 plays an essential role in stabilizing the AuNPs so that they are not removed from blood circulation.

Increase the penetration depth. At present, the most common PDT therapeutic window is between 600 and 950 nm. However, the excitation wavelength of most traditional PSs is lower than 780 nm. Short-wavelength light has poor tissue penetration due to its strong attenuation by the UV-visible absorption of oxyhemoglobin and tissue scattering.[86] As a result, the *in vivo* photodynamic effects are limited.[87,88] To address this problem, Yang *et al.* employed dual-modal PDT mediated by high-transmittance NIR light (Fig. 4A).[89] The authors co-loaded carbon dots (CDs) and graphitic carbon nitride (g-C_3N_4) onto ZIF-8 *via* stepwise water splitting and covered the surface of the nanoplatform with UCNPs through *in situ* growth. The addition of CDs to the g-C_3N_4 sheets enhanced the absorption intensity over the absorption range compared to g-C_3N_4 alone (Fig. 4B).[90] In this system, the g-C_3N_4 and CDs are continuously activated by the UV light emitted from the UCNPs, which transfer deep-penetrating low-energy NIR light to high-energy UV light upon irradiation with a 980 nm laser (Fig. 4C and D). The visible light produced by the CDs can activate g-C_3N_4 to produce ROS, thereby maximizing light utilization. Many two photon-excited PSs have been developed to overcome the difficulty in activating long-wavelength NIR light (>750 nm) *via* one-photon excitation and improve tissue penetration.[91,92] However, the combination of UCNPs with CDs and g-C_3N_4 can further increase the penetration depth and efficiency of the laser.

Multi-modal imaging-guided PDT. Although fluorescence imaging, a noninvasive and real-time imaging modality, can be induced by PSs during PDT, this technique is not commonly used in clinical settings at present.[93] Theranostic nanoprobes that can simultaneously realize traditional medical imaging and PDT have been reported. For example, Sun *et al.* reported a novel pH-responsive magnetic resonance imaging (MRI) drug delivery system (BSA–MnO_2/Ce6@ZIF-8).[94] This system was formed *via* a one-pot route in which Ce6 was integrated into the ZIF-8 matrix followed by loading bovine serum albumin (BSA)–MnO_2 NPs with CAT-like activity on the surface of ZIF-8. MnO_2 generated Mn^{2+} by reacting with H_2O_2 in the acidic TME for $T1$-weighted MRI (Fig. 5A and B).[95,96] Meanwhile, the concentration

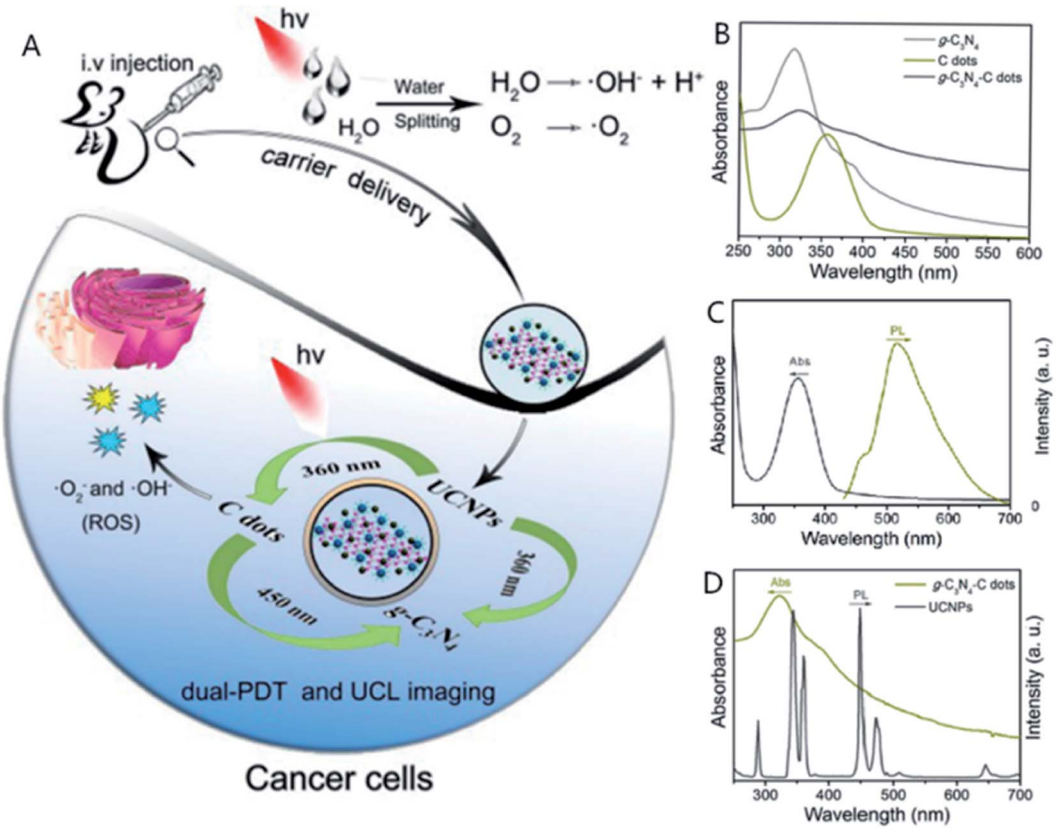

Fig. 4 (A) Schematic of the anti-tumor mechanism of UCNPs-g-C_3N_4–CDs@ZIF-8. (B) UV-visible absorbance spectra of g-C_3N_4, CDs, and g-C_3N_4–CDs. (C) The emission spectrum upon 360 nm excitation and the absorption spectrum of CDs. (D) The emission spectrum of UCNPs under 980 nm laser excitation and the absorption spectrum of the g-C_3N_4–CDs PS. [This figure has been reproduced from ref. 89 with permission from American Chemical Society, copyright 2017].

of O_2 increased with H_2O_2 decomposition (Fig. 5C). This strategy integrates MRI with Ce6-mediated fluorescence imaging based on O_2 production to achieve multi-modal imaging-guided PDT.

Photoacoustic (PA) imaging has become a promising technique for deep tumors due to the great acoustic depth of penetration and optical resolution.[97,98] Qu *et al.* designed ZIF-8–IR820–MnPc–HA (ZIMH) NPs that combined PA imaging with NIR-II fluorescence imaging to improve the visualization and localization of tumors (Fig. 6).[99] To form the ZIMH NPs, IR820 and MnPc were encapsulated uniformly in the porous structure of ZIF-8 to reduce quenching and produce $^1O_2$ under 808 nm irradiation. This multi-modal imaging-guided PDT provides a new strategy for the early and accurate diagnosis and treatment of tumors.

Synergistic PDT nanoplatforms

Synergistic PDT and chemotherapy. Chemotherapy is one of the most widely used treatment modalities. However, the multiple disadvantages of chemotherapeutic drugs, including serious side effects, drug tolerance, and nonselective drug distribution and release, severely hinder their practical application.[100,101] Currently, most clinical-stage nanomedicines for chemotherapy are based on liposomes.[7] However, considering the hypersensitivity and immune suppression of liposomes, nMOFs and particularly ZIF-8 may be better carriers for chemotherapeutic drugs because of their high biodegradability and low biological toxicity. Since Chen *et al.* first synthesized photo-chemo combination NPs (g-C_3N_4@ZIF-8),[102] other reports have indicated that chemotherapeutic drugs including

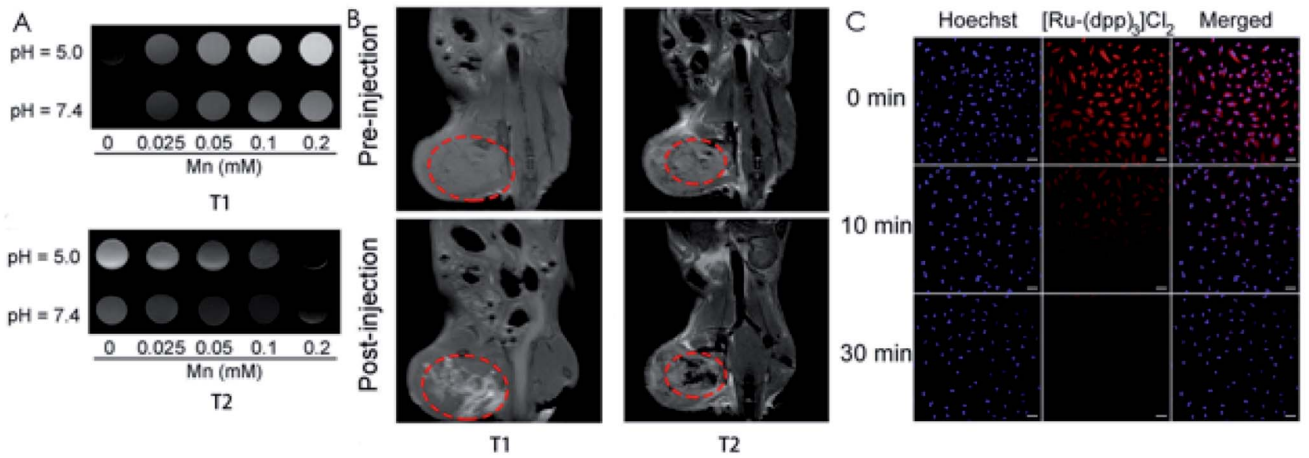

Fig. 5 (A) *T*1-and *T*2-weighted MRI images of NPs at pH 5.0 and 7.4. (B) *In vivo T*1-and *T*2-weighted MRI images before and after injection with NPs. (C) CLSM images of HeLa cells incubated with BSA–MnO_2/Ce6@ZIF-8 for different times after staining with Hoechst 33342 and [Ru-(dpp)$_3$]Cl_2. [This figure has been reproduced from ref. 94 with permission from American Chemical Society, copyright 2019].

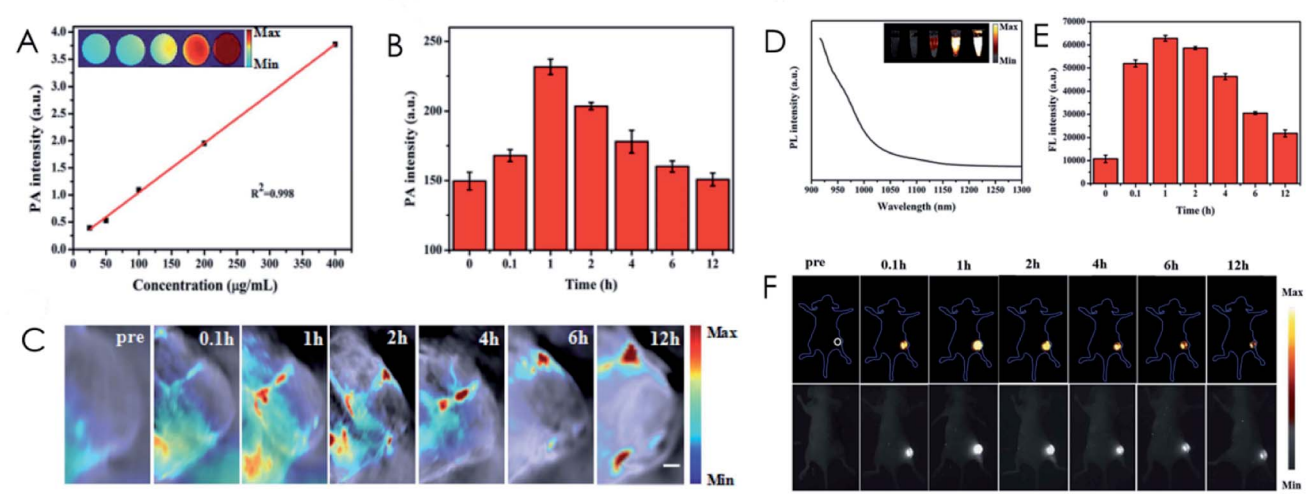

Fig. 6 The linear relationships between the PA (A) and fluorescence (D) intensity and the ZIMH concentration. PA (B) and fluorescence (E) intensity of the tumor sites of mice *in vivo* at different times after the injection of ZIMH. PA (C) and fluorescence (F) images of the tumors at different time points after ZIMH injection. [This figure has been reproduced from ref. 99 with permission from Royal Society of Chemistry, copyright 2021].

doxorubicin (DOX) can be co-encapsulated with PSs in ZIF-8. Gold nanocluster (AuNC) PSs with the capacity for ROS generation have also realized efficient photo-chemo effects.[103,104] CAT and CAT-like materials including MnO_2 nanodots can be further introduced to relieve hypoxia during photo-chemotherapy *via* the catalysis of endogenous H_2O_2.[105] In a photo-chemotherapeutic nanosystem containing two kinds of MOFs, Ren *et al.* utilized ZIF-67 as an analog of CAT to encapsulate DOX.[106]

Amphiphilic block copolymer was combined with ZIF-8 as a drug carrier to construct a pH/H_2O_2 dual-controlled associative PDT and chemotherapy nanoplatform (termed BCP/Cit-Fe(III)@ZIF-8).[107,108] To form this nanoplatform, DOX and poly(L-lactic acid)-*block*-poly(sodium 4-styrenesulfonate) (BCP) were self-assembled in aqueous solution followed by the attachment of ferric citrate [Cit-Fe(III)] through electrostatic interaction. Finally, ZIF-8 was grown on the surfaces of the NPs. Under co-stimulation by H_2O_2 and visible light and the catalysis of Cit-Fe(III), sufficient ROS were released (Fig. 7).[109–111] At the same time, the ROS were oxidized and decomposed sulfonate-containing polymeric vesicles, causing the encapsulated DOX to spread into ZIF-8. Under low pH, ZIF-8 disintegrated to achieve controlled drug release and an excellent anti-cancer effect.

In another photo-chemotherapy nanosystem, Qin and his colleagues loaded Gd-doped silicon NPs (Si–Gd NPs) into the ZIF-8 matrix to endow it with MRI properties.[112] In this system, the combination of MRI/fluorescence imaging modalities and folic acid polyethylene glycol-maleimide (MaL-PEG-FA) as a cancer target molecule allows for a precise treatment effect.[113]

Synergistic PDT and photothermal therapy (PTT). PTT is an alternative approach to phototherapy in which photothermal agents (PTAs) are used to convert NIR light into heat.[114] PTT usually employs NIR light with a longer wavelength than PDT, resulting in deeper penetration.[115] PTAs and PSs can be co-loaded into ZIF-8 using appropriate synthetic methods to form photothermal and photodynamic systems.[48,116] Yang *et al.* co-encapsulated Fe_3O_4 nanocrystals and $Au_{25}(SR)_{18}^-$ clusters in ZIF-8 as PTAs to produce hyperthermal effects and realize MRI.[117] The ultrasmall $Au_{25}(SR)_{18}^-$ clusters loaded on Fe_3O_4/ZIF-8-Au_{25} enhanced the photothermal effect while producing singlet oxygen.[48,116] Another reported co-delivery method is to make ZIF-8 encapsulating small molecule PSs grow *in situ* on the surfaces of large-molecule PTAs to overcome the small pore diameter of ZIF-8.[118]

In addition, ZIF-8 has been directly pyrolyzed to obtain ZIF-8-derived carbon nanoparticles that served as both a PTA and PS rather than using two different drugs.[119]

Synergistic PDT and chemodynamic therapy (CDT). Previous studies have demonstrated that O_2 can be absorbed and stored by ZIF-8.[120] Compared with other MOFs with coordination-unsaturated Cu sites (HKUST-1, MCM-152), unmodified ZIF-8 has poor O_2 storage capacity.[121–123] To address this issue, Cu^{2+} was doped into the ZIF-8 matrix to construct a pH-responsive nanoplatform (O_2–Cu/ZIF-8@Ce6/ZIF-8@F127, designated as OCZCF) to enhance O_2 adsorption (Fig. 8A).[71] The OCZCF nanoplatform can carry O_2 by itself *via* Cu^{2+}-doped ZIF-8 (Cu/ZIF-8), and the quantity of O_2 loaded in Cu/ZIF-8 is twice that loaded in the ordinary ZIF-8 matrix (Fig. 8B). In addition, Cu^{2+} and the byproduct Cu^+ can participate in Fenton-like reactions to realize CDT, which transforms intracellular H_2O_2 into highly cytotoxic hydroxyl radicals (•OH) to eliminate tumor cells containing excessive glutathione (GSH) (Fig. 8C).[124,125] Based on experimental results, OCZCF is a promising, highly efficient nanoplatform for synergetic PDT and CDT (Fig. 8D).

Synergistic PDT and starvation therapy (ST). Cascade reactions can be employed to amplify the anticancer efficacy of existing treatments.[126] Glucose oxidase (GOx), a popular drug

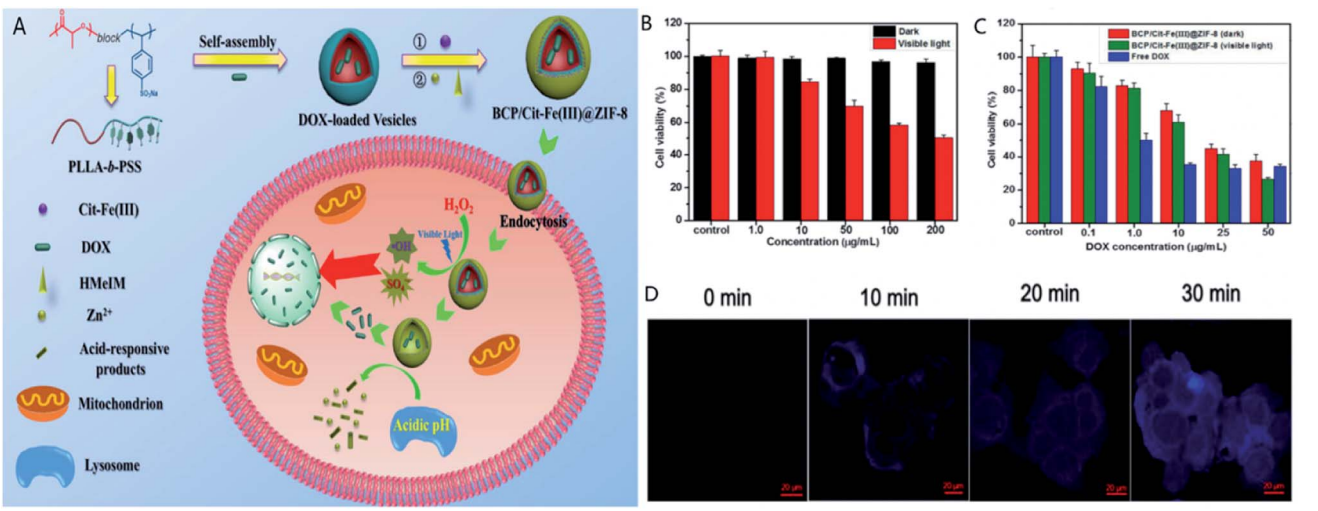

Fig. 7 (A) Anti-tumor mechanism of BCP/Cit-Fe(III)@ZIF-8 *in vivo*. (B) Cell viability in the presence of different concentrations of the nanoplatform in the dark and under visible light. (C) Cell viability in the presence of various DOX concentrations after different treatments. (D) Intracellular hydroxyl radicals detected by incubating MCF-7 cells with coumarin under visible light. [This figure has been reproduced from ref. 108 with permission from American Chemical Society, copyright 2019].

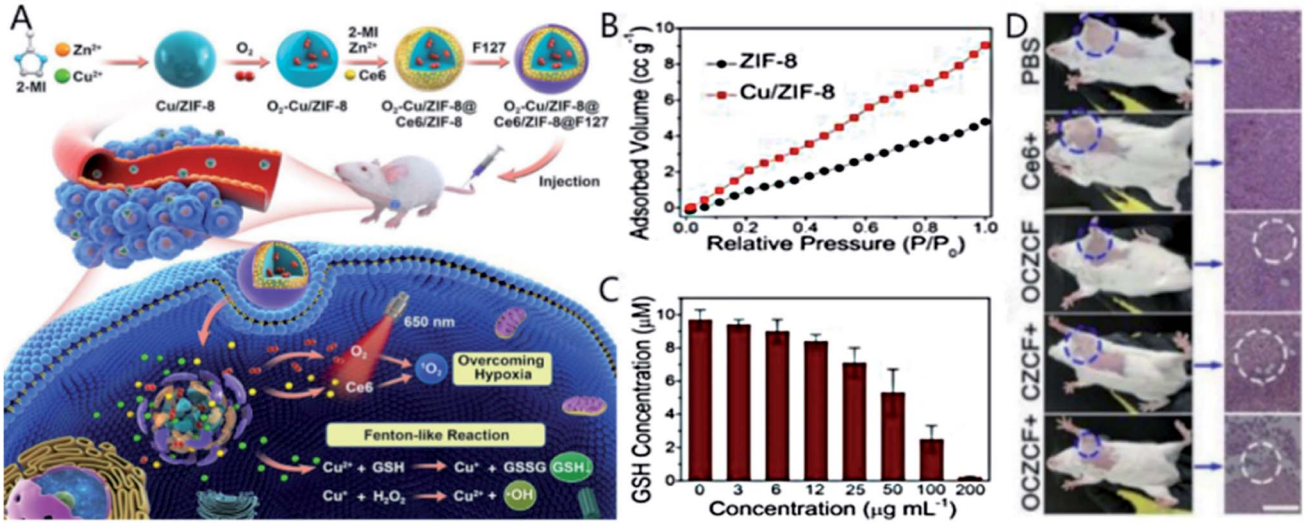

Fig. 8 (A) Schematic illustration of the synthesis and therapeutic mechanism of OCZCF. (B) O_2 adsorption isotherms of ZIF-8 and Cu/ZIF-8. (C) The correlation between GSH concentration and OCZCF concentration. (D) Photographs of mice who received different treatments. [This figure has been reproduced from ref. 71 with permission from American Chemical Society, copyright 2019].

used for ST, catalyzes the oxidization of glucose into gluconic acid and H_2O_2.[127] As the catalysis of GOx causes the TME to become more acidic and hypoxic, GOx-based nanocomposites usually have the capacity for cascade reaction.[128,129] You *et al.* constructed a core–shell, self-driven UCNPs/TAPP@ZIF-8@catalase nanomotors and loaded GOx and CAT on their surfaces.[73] CAT catalyzed the decomposition of GOx-catalyzed and endogenous H_2O_2 to provide a driving force for GOx catalysis. The experimental data indicated that the nanomotors generated positive feedback into the therapeutic process under cascade reactions driven by two enzymes, vastly improving the synergistic PDT and ST effect. While the combination of GOx and CAT, 2,4-dinitrobenzenesulfonyl chloride-quenched porphyrin (TPP–DNB) as a GSH-activated generator was loaded into ZIF-8.[130,131] ZIF-8 and TPP-DNB realized the drug release at low pH and antitumor treatment activated by excessive GSH in the TME.

Synergistic PDT and protein therapy. Hydrolysis and denaturation *in vivo* and the immunogenicity of proteins hinder the clinical applications of protein therapy.[132,133] Biomineralization is a useful strategy to combine biomacromolecules, including therapeutic proteins, and MOFs.[38] Cytochrome c (Cyt c) and Ce6 were encapsulated together into ZIF-8 *via* a one-pot biomimetic mineralization strategy to convey and protect therapeutic proteins.[134] Cyt c can induce tumor cell apoptosis and retain the peroxidase/CAT-like activity under hypoxic conditions to alleviate tumor hypoxia and enhance PDT.[135]

Synergistic PDT and gene therapy. Although a promising tumor therapy, gene therapy, which can induce gene silencing, antisense therapy, RNA interference, gene and genome editing, has been limited to inefficient delivery to tumor tissue. Metallic NPs, silica NPs, carbon-derived NPs, liposomes, and polymeric NPs have been designed for gene therapy.[136,137] However, the cytotoxicity, biocompatibility, biodegradability, and anaphylactic effect of these NPs require further study. Wang and colleagues loaded Ce6-modified DNAzymes as a gene therapy agent into ZIF-8 (ref. 138 and 139) to achieved simultaneous gene therapy and PDT. Under low pH, the release of Ce6-DNAzyme was accompanied by the disintegration of ZIF-8, and the byproduct Zn^{2+} acted as a cofactor of DNAzyme to overcome the low efficiency of intracellular delivery and insufficient supply of cofactor.[140]

Synergistic PDT, PTT, and chemotherapy. ZIF-8 was reported to be carbonized to produce fluorescent carbon nanodots for biosensing *via* low-temperature annealing.[141] ZIF-8-derived nanomaterials are still rarely studied in cancer therapies.[142] Sui *et al.* designed a simple multi-functional nanoplatform (FeNC@PAA) based on a ZIF-8 derivative for cooperative tri-modal therapy.[143] The precursor ZIF-8 was simply pyrolyzed to synthesize Fe–N co-doped carbon (FeNC) NPs (Fig. 9A). Metal–nitrogen–carbon NPs derived from MOFs, including Zn–N–C nanomaterials synthesized *via* the pyrolysis of ZIF-8, have porphyrin-like zinc centers and can be used as PSs for PDT.[144] The porphyrin-like metal center of the FeNC@PAA nanoplatform can be used for PDT[145] and boost the Fenton-like reaction to produce ·OH for CDT *via* Fe^{2+} (Fig. 9B). Experimental results suggest that FeNC@PAA has a high NIR absorption rate and a photothermal conversion efficiency of up to 29.15% (Fig. 9C).

Synergistic PDT, CDT, and ST. ST-triggered glucose decomposition consumes O_2 at tumor sites while providing H_2O_2, which is necessary for CDT but limits PDT. MnO_2 can both provide O_2 by mimicking CAT and mediate the Fenton reaction *via* Mn^{2+} to facilitate simultaneous PDT and CDT. In consideration of this characteristic, Zhang *et al.* combined MnO_2 and GOx to construct intelligent cascade nanoparticles with O_2 production and GSH/glucose consumption capacity CGZPM (Fig. 10).[146] In this design, ZIF-8 not only serves as a nanocarrier of Ce6 and Gox, it also directly initiates the surface polymerization of dopamine to prevent the premature release of Ce6 and

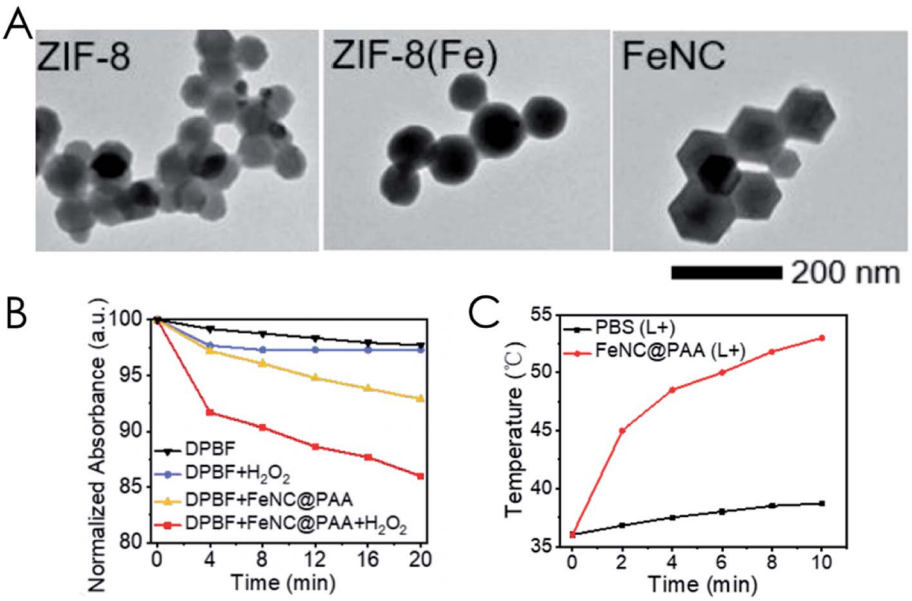

Fig. 9 (A) TEM images of ZIF-8 (Zn), ZIF-8 (Fe/Zn), and FeNC NPs. (B) Decay curves of DPBF-normalized absorption at 410 nm under different conditions and 808 nm laser irradiation (0.5 W cm^{-2}). (C) Temperature change of the tumor site during irradiation (0.3 W cm^{-2}, 10 min). [This figure has been reproduced from ref. 143 with permission from American Chemical Society, copyright 2021].

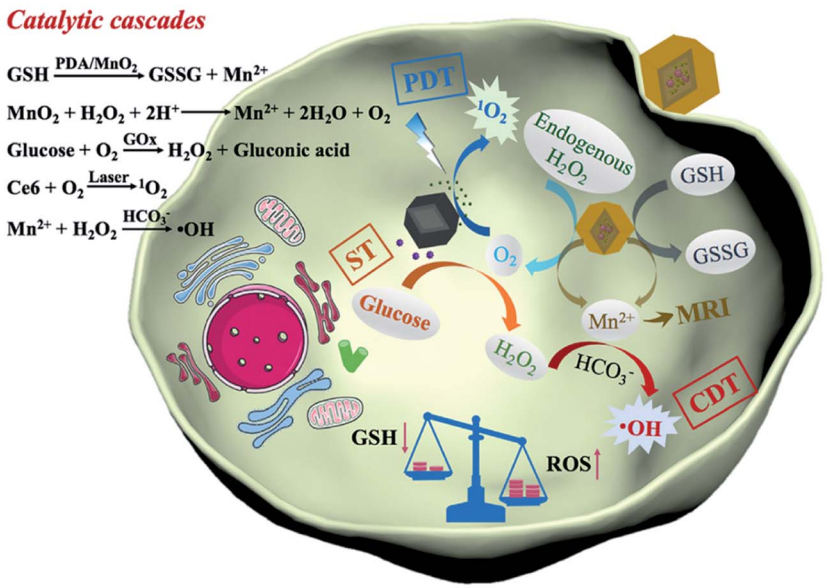

Fig. 10 Schematic of the reaction mechanism of CGZPM *in vivo*. [This figure has been reproduced from ref. 146 with permission from Elsevier Inc., copyright 2021].

GOx. As a therapeutic nanosystem, CGZPM reached the goal of overcoming limitations of hypoxia and GSH overexpression in TME and conducting MRI.

Synergistic PDT, CDT, and chemotherapy. Different kinds of drugs loaded onto the same carrier may interact with each other, affecting the drug efficacy. Therefore, the use of various carriers to transport different drugs in a drug delivery system can be considered in combined anticancer treatments. Wu *et al.* built core–shell tri-modal therapeutic nanoparticles (MIL-88-ICG@ZIF-8-DOX) based on MIL-88 as the core and ZIF-8 as the shell.[147] MIL-88 can intelligently adjust the aperture size to adapt to the size of indocyanine green (ICG), thereby improving the drug stability without harming the framework topology.[148,149] In addition, the iron ions in MIL-88 can be used for CDT and also continuously generate O_2 to enhance the efficacy of PDT through a Fenton-like reaction. Another method of carrying ICG/DOX is with the help of hollow porphyrinic MOF (H-PMOF) NPs which were

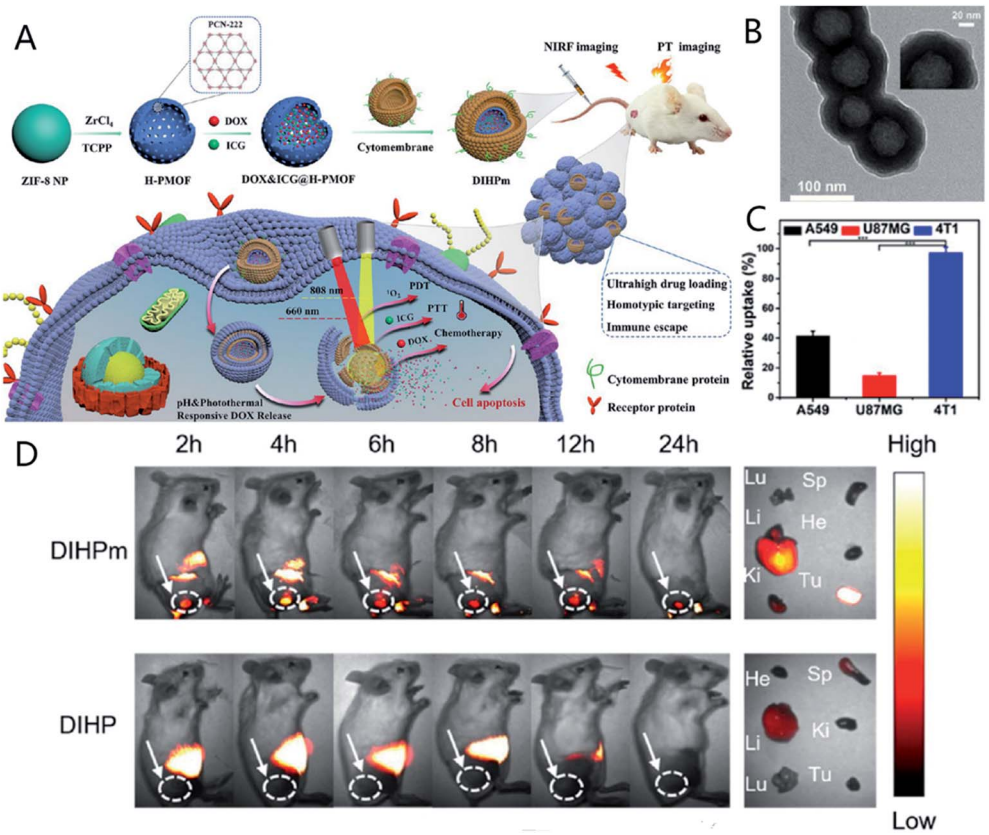

Fig. 11 (A) Schematic of the synthesis and reaction mechanism of DIHPm. (B) TEM images of DIHPm. (C) Relative cellular uptake of DIHPm against various cell lines (A549, U87MG, and 4T1). (D) Fluorescence images of 4T1 tumor-bearing mice at different timepoints after the intravenous injection of DIHPm or DIHP. [This figure has been adapted from ref. 150 with permission from American Chemical Society, copyright 2021].

synthesized by a ZIF-8 template used to load ICG (Fig. 11A and B).[150] The loading capacity of H-PMOF for DOX and ICG was over six times that of non-hollow porphyrinic MOF NPs. The nanoplatform was also covered with Mem to provide homologous tumor-targeting and immune-escaping ability for precise synergistic therapy (Fig. 11C and D).

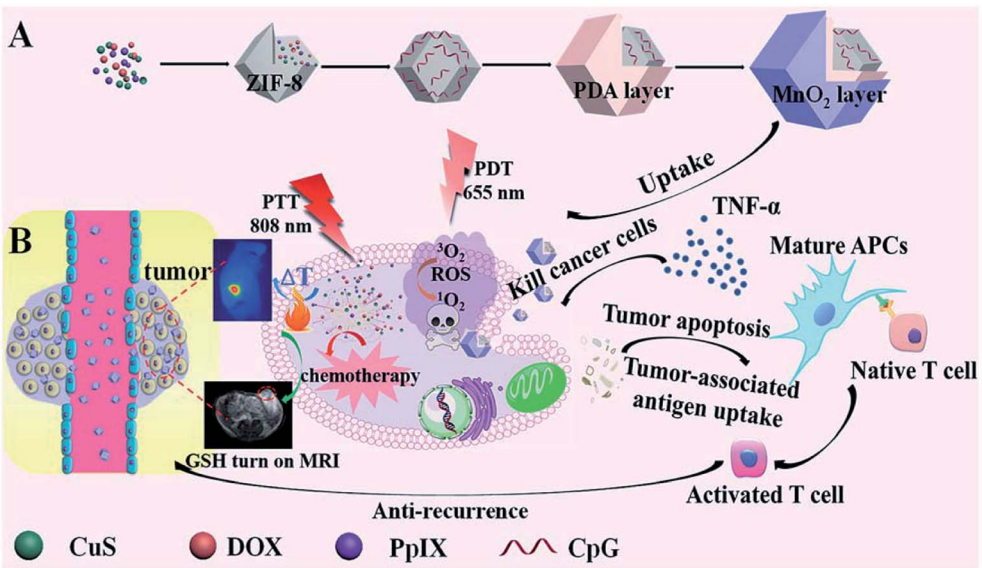

Fig. 12 Schematic diagram of the synthesis and applications of CuZPMn@CpG nanocomposite. [This figure has been reproduced from ref. 151 with permission from Royal Society of Chemistry, copyright 2018].

Synergistic PDT, PTT, chemotherapy, and immunotherapy. The synthesis of nanomaterials that integrate multiple agents into therapeutic multifunctional NPs is limited by the interactions between different drugs and the complex synthetic procedures. Using a simple one-pot route, Yang *et al.* co-loaded the ZIF-8 matrix with a variety of therapeutic agents, including PpIX for PDT, CuS NPs for PTA, and DOX for chemotherapy, for synergistic PDT, PTT, and chemotherapy (Fig. 12).[151] Negative cytosine–phosphate guanine (CpG), which is recognized by Toll-like receptor 9 (TLR9),[152] was adsorbed onto the surface of positive ZIF-8 *via* electrostatic interactions for immunotherapy, which is a promising auxiliary therapy for controlling cancer recurrence and metastasis.[153,154] A polydopamine (PDA) layer was then grown to enhance the PTT effect and protect negative CpG. The system was covered by an outer layer of MnO_2, which served as a GSH-responsive MRI contrast agent. Experiments confirmed that this synergistic nanoplatform achieved MRI-guided multi-modality therapy and inhibited tumor recurrence and metastasis *via* immune memory.

Conclusion and outlook

Multifunctional nanoplatforms based on ZIF-8 and its derivatives have shown outstanding application prospects in PDT. The porosity and easy modification of the ZIF-8 skeleton largely overcome the low photosensitizer efficiency and hypoxia in conventional PDT. The reaction of ZIF-8 in acidic conditions also contributes to the precise release of drugs in tumor sites. ZIF-8 can also be used as an intermediary to realize synergistic PDT and other anti-tumor therapies by delivering different small-molecule therapeutic agents. However, ZIF-8 still has some weaknesses.

(1) As a carrier in PDT, ZIF-8 still needs to face challenges of low accumulation at tumor sites and unclear metabolic mechanisms *in vivo*. Without any surface modification, ZIF-8 has a short blood circulation time and low accumulation in tumor cells.[155] Thus, modifiers must be added to ZIF-8 to overcome these limitations. In addition, most studies on ZIF-8-based nanomaterials have not explored the metabolic mechanisms and long-term side effects, and the effects of these nanomaterials on the immune system remain unknown.

(2) Although zinc, a component of ZIF-8, is one of the vital transition metal in organisms and essential for life, the accumulation of zinc in cells can damage the cells.[156] Chen *et al.* thought that smaller ZIF-8 nanoplatforms would lead to more zinc accumulation. Although more zinc can provide more ROS, excess zinc can result in cytotoxicity.[157] Further studies are needed to design ZIF-8 nanoplatforms with suitable sizes to decrease toxicity to normal tissues.

(3) The design of synergistic therapeutic nanoplatforms based on ZIF-8 remains complicated. Although there is a universal one-pot route to encapsulate small molecules, a simple and versatile way to integrate multiple therapeutic drugs into nanosystems has not been identified.

(4) Most ZIF-8 nanoplatforms for PDT are designed to alleviate hypoxia and deliver PSs. Thus, low tissue penetration depth in PDT remains a problem. Future work could focus on designing better ZIF-8-based PSs to extend the excitation wavelength and increase the penetration depth in PDT.

(5) PDT based on ZIF-8 has been primarily studied at the cell level and/or animal level, and human clinical data are lacking. Whether these nanoplatforms can pass rigorous clinical evaluation is still uncertain. We anticipate that researchers can overcome the remaining problems to build ZIF-8-based nanoplatforms for application in clinical treatment in the near future.

Author contributions

Wen Kang: conceptualization, methodology, software, validation, formal analysis, investigation, resources, data curation, writing – original draft, writing – review & editing.

Ying Tian: conceptualization, methodology, software, validation, data curation, writing – original draft, writing – review & editing, project administration, funding acquisition.

Ying Zhao: software, validation, formal analysis, resources, data curation, writing – review & editing, visualization, project administration, funding acquisition.

Xindao Yin: conceptualization, software, investigation, resources, data curation, writing – review & editing, visualization, supervision, project administration, funding acquisition.

Zhaogang Teng: conceptualization, methodology, validation, investigation, writing – review & editing, supervision, project administration.

Conflicts of interest

The authors declare that they have no known competing financial interests or personal relationships that could have appeared to influence the work reported in this article.

Acknowledgements

This work was supported by National Natural Science Foundation of China (grant numbers 81901806 and 81971681).

References

1 R. L. Siegel, K. D. Miller and A. Jemal, *Ca-Cancer J. Clin.*, 2020, **70**, 7–30.
2 M. Jablonická, L. Žideková and B. Mladosievičová, *Vnitr. Lek.*, 2021, **67**, 26–31.
3 M. Dominguez and R. Malani, *Curr. Pain Headache Rep.*, 2021, **25**, 33.
4 P. Iglesias, J. C. Sánchez and J. J. Díez, *Pituitary*, 2021, **24**, 630–643.
5 J. Yu, Y. Ju, L. Zhao, X. Chu, W. Yang, Y. Tian, F. Sheng, J. Lin, F. Liu, Y. Dong and Y. Hou, *ACS Nano*, 2016, **10**, 159–169.
6 O. C. Farokhzad and R. Langer, *ACS Nano*, 2009, **3**, 16–20.
7 J. Shi, P. W. Kantoff, R. Wooster and O. C. Farokhzad, *Nat. Rev. Cancer*, 2017, **17**, 20–37.
8 F. Wang, C. Li, J. Cheng and Z. Yuan, *Int. J. Environ. Res. Public Health*, 2016, **13**, 1182.

9 J. L. Paris, A. Baeza and M. Vallet-Regí, *Expert Opin. Drug Delivery*, 2019, **16**, 1095–1112.
10 M. Yokoyama, *J. Drug Targeting*, 2014, **22**, 576–583.
11 L. Larue, B. Myrzakhmetov, A. Ben-Mihoub, A. Moussaron, N. Thomas, P. Arnoux, F. Baros, R. Vanderesse, S. Acherar and C. Frochot, *Pharmaceuticals*, 2019, **12**, 163.
12 N. Thotakura, P. Parashar and K. Raza, *Expert Opin. Drug Metab. Toxicol.*, 2021, **17**, 323–332.
13 H.-C. Zhou, J. R. Long and O. M. Yaghi, *Chem. Rev.*, 2012, **112**, 673–674.
14 J. L. C. Rowsell and O. M. Yaghi, *Microporous Mesoporous Mater.*, 2004, **73**, 3–14.
15 K. K. Tanabe, Z. Wang and S. M. Cohen, *J. Am. Chem. Soc.*, 2008, **130**, 8508–8517.
16 C. Wang, D. Liu and W. Lin, *J. Am. Chem. Soc.*, 2013, **135**, 13222–13234.
17 M. Eddaoudi, J. Kim, N. Rosi, D. Vodak, J. Wachter, M. O'Keeffe and O. M. Yaghi, *Science*, 2002, **295**, 469–472.
18 J. Li, P. M. Bhatt, J. Li, M. Eddaoudi and Y. Liu, *Adv. Mater.*, 2020, **32**, 2002563.
19 W.-Q. Tang, J.-Y. Xu and Z.-Y. Gu, *Chem.–Asian J.*, 2019, **14**, 3462–3473.
20 H. Wan, Y. Wang, J. Chen, H. M. Meng and Z. Li, *Mikrochim. Acta*, 2021, **188**, 130.
21 Y.-B. Huang, J. Liang, X.-S. Wang and R. Cao, *Chem. Soc. Rev.*, 2016, **46**, 126–157.
22 L. Du, W. Chen, P. Zhu, Y. Tian, Y. Chen and C. Wu, *Biotechnol. J.*, 2021, **16**, 1900424.
23 J. W. M. Osterrieth and D. Fairen-Jimenez, *Biotechnol. J.*, 2021, **16**, 2000005.
24 D. Gao, Y. Gao, J. Shen and Q. Wang, *Photodiagn. Photodyn. Ther.*, 2020, **32**, 102026.
25 M.-X. Wu and Y.-W. Yang, *Adv. Mater.*, 2017, **29**, 1606134.
26 K. S. Park, Z. Ni, A. P. Côté, J. Y. Choi, R. Huang, F. J. Uribe-Romo, H. K. Chae, M. O'Keeffe and O. M. Yaghi, *Proc. Natl. Acad. Sci. U. S. A.*, 2006, **103**, 10186–10191.
27 C. Andreini, L. Banci, I. Bertini and A. Rosato, *J. Proteome Res.*, 2006, **5**, 3173–3178.
28 J. Zhuang, C.-H. Kuo, L.-Y. Chou, D.-Y. Liu, E. Weerapana and C.-K. Tsung, *ACS Nano*, 2014, **8**, 2812–2819.
29 J. Yan, C. Liu, Q. Wu, J. Zhou, X. Xu, L. Zhang, D. Wang, F. Yang and H. Zhang, *Anal. Chem.*, 2020, **92**, 11453–11461.
30 H.-Y. Cho, J. Kim, S.-N. Kim and W.-S. Ahn, *Microporous Mesoporous Mater.*, 2013, **169**, 180–184.
31 Q. Shi, Z. Chen, Z. Song, J. Li and J. Dong, *Angew. Chem., Int. Ed. Engl.*, 2011, **50**, 672–675.
32 F. Hillman, J. Brito and H.-K. Jeong, *ACS Appl. Mater. Interfaces*, 2018, **10**, 5586–5593.
33 R. Banerjee, A. Phan, B. Wang, C. Knobler, H. Furukawa, M. O'Keeffe and O. M. Yaghi, *Science*, 2008, **319**, 939–943.
34 P. J. Beldon, L. Fábián, R. S. Stein, A. Thirumurugan, A. K. Cheetham and T. Friščić, *Angew. Chem., Int. Ed. Engl.*, 2010, **49**, 9640–9643.
35 M. Faustini, J. Kim, G.-Y. Jeong, J. Y. Kim, H. R. Moon, W.-S. Ahn and D.-P. Kim, *J. Am. Chem. Soc.*, 2013, **135**, 14619–14626.
36 Y.-R. Lee, M.-S. Jang, H.-Y. Cho, H.-J. Kwon, S. Kim and W.-S. Ahn, *Chem. Eng. J.*, 2015, **271**, 276–280.
37 A. Dhakshinamoorthy, A. M. Asiri and H. Garcia, *Dalton Trans.*, 2020, **49**, 11059–11072.
38 C. Chu, M. Su, J. Zhu, D. Li, H. Cheng, X. Chen and G. Liu, *Theranostics*, 2019, **9**, 3134–3149.
39 Y. Wang, X. Dai, Y. Zhan, X. Ding, M. Wang and X. Wang, *Int. J. Biol. Macromol.*, 2019, **137**, 77–86.
40 C. Hu, Y. Yu, S. Chao, H. Zhu, Y. Pei, L. Chen and Z. Pei, *Molecules*, 2021, **26**, 3878.
41 O. Karagiaridi, M. B. Lalonde, W. Bury, A. A. Sarjeant, O. K. Farha and J. T. Hupp, *J. Am. Chem. Soc.*, 2012, **134**, 18790–18796.
42 M. C. DeRosa and R. J. Crutchley, *Coord. Chem. Rev.*, 2002, **233–234**, 351–371.
43 M. L. Agarwal, M. E. Clay, E. J. Harvey, H. H. Evans, A. R. Antunez and N. L. Oleinick, *Cancer Res.*, 1991, **51**, 5993–5996.
44 P. Vijayaraghavan, C.-H. Liu, R. Vankayala, C.-S. Chiang and K. C. Hwang, *Adv. Mater.*, 2014, **26**, 6689–6695.
45 D. Kessel and N. L. Oleinick, *Photochem. Photobiol.*, 2018, **94**, 213–218.
46 D. Van Straten, V. Mashayekhi, H. S. De Bruijn, S. Oliveira and D. J. Robinson, *Cancers*, 2017, **9**, 19.
47 W. M. Star, H. P. A. Marijnissen, A. E. van den Berg-Blok, J. A. C. Versteeg, K. A. P. Franken and H. S. Reinhold, *Cancer Res.*, 1986, **46**, 2532–2540.
48 D. Yang, G. Yang, S. Gai, F. He, G. An, Y. Dai, R. Lv and P. Yang, *Nanoscale*, 2015, **7**, 19568–19578.
49 S. Kwiatkowski, B. Knap, D. Przystupski, J. Saczko, E. Kędzierska, K. Knap-Czop, J. Kotlińska, O. Michel, K. Kotowski and J. Kulbacka, *Biomed. Pharmacother.*, 2018, **106**, 1098–1107.
50 I. S. Mfouo-Tynga, L. D. Dias, N. M. Inada and C. Kurachi, *Photodiagn. Photodyn. Ther.*, 2021, **34**, 102091.
51 R. Baskaran, J. Lee and S.-G. Yang, *Biomater. Res.*, 2018, **22**, 25.
52 S. Wang, X. Wang, L. Yu and M. Sun, *Photodiagn. Photodyn. Ther.*, 2021, **34**, 102254.
53 D. Xu, Y. You, F. Zeng, Y. Wang, C. Liang, H. Feng and X. Ma, *ACS Appl. Mater. Interfaces*, 2018, **10**, 15517–15523.
54 M.-R. Song, D.-Y. Li, F.-Y. Nian, J.-P. Xue and J.-J. Chen, *J. Mater. Sci.*, 2018, **53**, 2351–2361.
55 A. Narumi, R. Rachi, H. Yamazaki, S. Kawaguchi, M. Kikuchi, H. Konno, T. Osaki, Y. Okamoto, X. Shen, T. Kakuchi, H. Kataoka, A. Nomoto, T. Yoshimura and S. Yano, *ACS Omega*, 2021, **6**, 7023–7033.
56 R. Bonnett, R. D. White, U. J. Winfield and M. C. Berenbaum, *Biochem. J.*, 1989, **261**, 277–280.
57 X. Fu, Z. Yang, T. Deng, J. Chen, Y. Wen, X. Fu, L. Zhou, Z. Zhu and C. Yu, *J. Mater. Chem. B*, 2020, **8**, 1481–1488.
58 K. Valachová and L. Šoltés, *Molecules*, 2021, **26**, 1195.
59 M. Hassn Mesrati, S. E. Syafruddin, M. A. Mohtar and A. Syahir, *Biomolecules*, 2021, **11**, 1850.
60 G. Mattheolabakis, L. Milane, A. Singh and M. M. Amiji, *J. Drug Targeting*, 2015, **23**, 605–618.

61 G. Borland, J. A. Ross and K. Guy, *Immunology*, 1998, **93**, 139–148.
62 P. Teriete, S. Banerji, M. Noble, C. D. Blundell, A. J. Wright, A. R. Pickford, E. Lowe, D. J. Mahoney, M. I. Tammi, J. D. Kahmann, I. D. Campbell, A. J. Day and D. G. Jackson, *Mol. Cell*, 2004, **13**, 483–496.
63 D.-H. Wan, B.-Y. Zheng, M.-R. Ke, J.-Y. Duan, Y.-Q. Zheng, C.-K. Yeh and J.-D. Huang, *Chem. Commun.*, 2017, **53**, 4112–4115.
64 D. Chen, M. Suo, J. Guo, W. Tang, W. Jiang, Y. Liu and Y. Duo, *Adv. Healthcare Mater.*, 2021, **10**, 2001577.
65 M. Benej, X. Hong, S. Vibhute, S. Scott, J. Wu, E. Graves, Q.-T. Le, A. C. Koong, A. J. Giaccia, B. Yu, C.-S. Chen, I. Papandreou and N. C. Denko, *Proc. Natl. Acad. Sci. U. S. A.*, 2018, **115**, 10756–10761.
66 S. Liu, H. Zhang, Y. Li, J. Liu, L. Du, M. Chen, R. T. K. Kwok, J. W. Y. Lam, D. L. Phillips and B. Z. Tang, *Angew. Chem., Int. Ed.*, 2018, **57**, 15189–15193.
67 J. Zou, Z. Yin, P. Wang, D. Chen, J. Shao, Q. Zhang, L. Sun, W. Huang and X. Dong, *Chem. Sci.*, 2018, **9**, 2188–2194.
68 Y. Wang, L. Shi, D. Ma, S. Xu, W. Wu, L. Xu, M. Panahandeh-Fard, X. Zhu, B. Wang and B. Liu, *ACS Nano*, 2020, **14**, 13056–13068.
69 L. Tang, X. Yang, Q. Yin, K. Cai, H. Wang, I. Chaudhury, C. Yao, Q. Zhou, M. Kwon, J. A. Hartman, I. T. Dobrucki, L. W. Dobrucki, L. B. Borst, S. Lezmi, W. G. Helferich, A. L. Ferguson, T. M. Fan and J. Cheng, *Proc. Natl. Acad. Sci. U. S. A.*, 2014, **111**, 15344–15349.
70 C.-Y. Shih, P.-T. Wang, W.-C. Su, H. Teng and W.-L. Huang, *Biomedicines*, 2021, **9**, 137.
71 Z. Xie, S. Liang, X. Cai, B. Ding, S. Huang, Z. Hou, P. a. Ma, Z. Cheng and J. Lin, *ACS Appl. Mater. Interfaces*, 2019, **11**, 31671–31680.
72 Q. Xu, G. Zhan, Z. Zhang, T. Yong, X. Yang and L. Gan, *Theranostics*, 2021, **11**, 1937–1952.
73 Y. You, D. Xu, X. Pan and X. Ma, *Appl. Mater. Today*, 2019, **16**, 508–517.
74 Q. You, K. Zhang, J. Liu, C. Liu, H. Wang, M. Wang, S. Ye, H. Gao, L. Lv, C. Wang, L. Zhu and Y. Yang, *Adv. Sci.*, 2020, **7**, 1903341.
75 H. Cheng, J.-Y. Zhu, S.-Y. Li, J.-Y. Zeng, Q. Lei, K.-W. Chen, C. Zhang and X.-Z. Zhang, *Adv. Funct. Mater.*, 2016, **26**, 7847–7860.
76 Y. Wang, Z. Luan, C. Zhao, C. Bai and K. Yang, *Eur. J. Pharm. Sci.*, 2020, **142**, 105136.
77 X. Zhen, P. Cheng and K. Pu, *Small*, 2019, **15**, e1804105.
78 H.-J. Cai, T.-T. Shen, J. Zhang, C.-F. Shan, J.-G. Jia, X. Li, W.-S. Liu and Y. Tang, *J. Mater. Chem. B*, 2017, **5**, 2390–2394.
79 F. Wang and X. Liu, *Chem. Soc. Rev.*, 2009, **38**, 976–989.
80 F. Auzel, *Chem. Rev.*, 2004, **104**, 139–174.
81 B. del Rosal and D. Jaque, *Methods Appl. Fluoresc.*, 2019, **7**, 022001.
82 Y. Huang, F. Qiu, R. Chen, D. Yan and X. Zhu, *J. Mater. Chem. B*, 2020, **8**, 3772–3788.
83 Y. Zou, S. Long, T. Xiong, X. Zhao, W. Sun, J. Du, J. Fan and X. Peng, *ACS Cent. Sci.*, 2021, **7**, 327–334.
84 Y.-C. Ma, Y.-H. Zhu, X.-F. Tang, L.-F. Hang, W. Jiang, M. Li, M. I. Khan, Y.-Z. You and Y.-C. Wang, *Biomater. Sci.*, 2019, **7**, 2740–2748.
85 W. He, Y.-T. Zhou, W. G. Wamer, X. Hu, X. Wu, Z. Zheng, M. D. Boudreau and J.-J. Yin, *Biomaterials*, 2013, **34**, 765–773.
86 J. R. Starkey, A. K. Rebane, M. A. Drobizhev, F. Meng, A. Gong, A. Elliott, K. McInnerney and C. W. Spangler, *Clin. Cancer Res.*, 2008, **14**, 6564–6573.
87 A. V. Kachynski, A. Pliss, A. N. Kuzmin, T. Y. Ohulchanskyy, A. Baev, J. Qu and P. N. Prasad, *Nat. Photonics*, 2014, **8**, 455–461.
88 C. Zhang, K. Zhao, W. Bu, D. Ni, Y. Liu, J. Feng and J. Shi, *Angew. Chem., Int. Ed.*, 2015, **54**, 1770–1774.
89 D. Yang, G. Yang, S. Gai, F. He, C. Li and P. Yang, *ACS Appl. Mater. Interfaces*, 2017, **9**, 6829–6838.
90 J. Liu, Y. Liu, N. Liu, Y. Han, X. Zhang, H. Huang, Y. Lifshitz, S. T. Lee, J. Zhong and Z. Kang, *Science*, 2015, **347**, 970–974.
91 J. F. Algorri, M. Ochoa, P. Roldán-Varona, L. Rodríguez-Cobo and J. M. López-Higuera, *Cancers*, 2021, **13**, 3484.
92 F. Bolze, S. Jenni, A. Sour and V. Heitz, *Chem. Commun.*, 2017, **53**, 12857–12877.
93 Y. Ji, C. Jones, Y. Baek, G. K. Park, S. Kashiwagi and H. S. Choi, *Adv. Drug Delivery Rev.*, 2020, **167**, 121–134.
94 Q. Sun, H. Bi, Z. Wang, C. Li, C. Wang, J. Xu, D. Yang, F. He, S. Gai and P. Yang, *ACS Appl. Mater. Interfaces*, 2019, **11**, 36347–36358.
95 P. Prasad, C. R. Gordijo, A. Z. Abbasi, A. Maeda, A. Ip, A. M. Rauth, R. S. DaCosta and X. Y. Wu, *ACS Nano*, 2014, **8**, 3202–3212.
96 D. Wang, N. Zhang, X. Jing, Y. Zhang, Y. Xu and L. Meng, *J. Mater. Chem. B*, 2020, **8**, 8271–8281.
97 X. Ge, Q. Fu, L. Bai, B. Chen, R. Wang, S. Gao and J. Song, *New J. Chem.*, 2019, **43**, 8835–8851.
98 A. B. E. Attia, G. Balasundaram, M. Moothanchery, U. S. Dinish, R. Bi, V. Ntziachristos and M. Olivo, *Photoacoustics*, 2019, **16**, 100144.
99 B. Qu, Y. Han, J. Li, Q. Wang, B. Zhao, X. Peng and R. Zhang, *RSC Adv.*, 2021, **11**, 5044–5054.
100 C. Maihöfner, I. Diel, H. Tesch, T. Quandel and R. Baron, *Support. Care Cancer*, 2021, **29**, 4223–4238.
101 P. Smith, A. Lavery and R. C. Turkington, *Best Pract. Res., Clin. Gastroenterol.*, 2020, **48–49**, 101691.
102 R. Chen, J. Zhang, Y. Wang, X. Chen, J. A. Zapien and C.-S. Lee, *Nanoscale*, 2015, **7**, 17299–17305.
103 L. Zhang, Y. Gao, S. Sun, Z. Li, A. Wu and L. Zeng, *J. Mater. Chem. B*, 2020, **8**, 1739–1747.
104 Y. Tao, M. Li, J. Ren and X. Qu, *Chem. Soc. Rev.*, 2015, **44**, 8636–8663.
105 W. Zhang, S. Li, X. Liu, C. Yang, N. Hu, L. Dou, B. Zhao, Q. Zhang, Y. Suo and J. Wang, *Adv. Funct. Mater.*, 2018, **28**, 1706375.
106 S.-Z. Ren, B. Wang, X.-H. Zhu, D. Zhu, M. Liu, S.-K. Li, Y.-S. Yang, Z.-C. Wang and H.-L. Zhu, *ACS Appl. Mater. Interfaces*, 2020, **12**, 24662–24674.
107 H. Phan, V. Taresco, J. Penelle and B. Couturaud, *Biomater. Sci.*, 2021, **9**, 38–50.

108 Z. Lei, Y. Ju, Y. Lin, X. Bai, W. Hu, Y. Wang, H. Luo and Z. Tong, *ACS Appl. Bio Mater.*, 2019, **2**, 3648–3658.
109 A. K. Jacob, R. S. Hotchkiss, S. L. DeMeester, M. Hiramatsu, I. E. Karl, P. E. Swanson, J. P. Cobb and T. G. Buchman, *Surgery*, 1997, **122**, 243–254.
110 X. Feng, Z. Wang, Y. Chen, T. Tao, F. Wu and Y. Zuo, *Ind. Eng. Chem. Res.*, 2012, **51**, 7007–7012.
111 Y. Chen, Z. Liu, Z. Wang, M. Xue, X. Zhu and T. Tao, *J. Hazard. Mater.*, 2011, **194**, 202–208.
112 Y.-T. Qin, H. Peng, X.-W. He, W.-Y. Li and Y.-K. Zhang, *ACS Appl. Mater. Interfaces*, 2019, **11**, 34268–34281.
113 A. DeCarlo, C. Malardier-Jugroot and M. R. Szewczuk, *Bioconjugate Chem.*, 2021, **32**, 512–522.
114 Y. J. Hou, X. X. Yang, R. Q. Liu, D. Zhao, C. X. Guo, A. C. Zhu, M. N. Wen, Z. Liu, G. F. Qu and H. X. Meng, *Int. J. Nanomed.*, 2020, **15**, 6827–6838.
115 S. Cui, D. Yin, Y. Chen, Y. Di, H. Chen, Y. Ma, S. Achilefu and Y. Gu, *ACS Nano*, 2013, **7**, 676–688.
116 H. Kawasaki, S. Kumar, G. Li, C. Zeng, D. R. Kauffman, J. Yoshimoto, Y. Iwasaki and R. Jin, *Chem. Mater.*, 2014, **26**, 2777–2788.
117 D. Liu, J. Li, C. Wang, L. An, J. Lin, Q. Tian and S. Yang, *Nanomedicine*, 2021, **32**, 102335.
118 J. Feng, W. Yu, Z. Xu and F. Wang, *Chem. Sci.*, 2020, **11**, 1649–1656.
119 P. Yang, Y. Tian, Y. Men, R. Guo, H. Peng, Q. Jiang and W. Yang, *ACS Appl. Mater. Interfaces*, 2018, **10**, 42039–42049.
120 B. Russell, J. Villaroel, K. Sapag and A. D. Migone, *J. Phys. Chem. C*, 2014, **118**, 28603–28608.
121 W. Cheng, H. Zhang, D. Luan and X. W. Lou, *Sci. Adv.*, 2021, **7**, eabg2580.
122 P. Z. Moghadam, T. Islamoglu, S. Goswami, J. Exley, M. Fantham, C. F. Kaminski, R. Q. Snurr, O. K. Farha and D. Fairen-Jimenez, *Nat. Commun.*, 2018, **9**, 1378.
123 J. B. DeCoste, M. H. Weston, P. E. Fuller, T. M. Tovar, G. W. Peterson, M. D. LeVan and O. K. Farha, *Angew. Chem., Int. Ed. Engl.*, 2014, **53**, 14092–14095.
124 C. Zhang, W. Bu, D. Ni, S. Zhang, Q. Li, Z. Yao, J. Zhang, H. Yao, Z. Wang and J. Shi, *Angew. Chem., Int. Ed.*, 2016, **55**, 2101–2106.
125 P. Kuppusamy, H. Li, G. Ilangovan, A. J. Cardounel, J. L. Zweier, K. Yamada, M. C. Krishna and J. B. Mitchell, *Cancer Res.*, 2002, **62**, 307–312.
126 Y. Sun, X. Ma and H. Hu, *Int. J. Mol. Sci.*, 2021, **22**, 5698.
127 L.-H. Fu, C. Qi, J. Lin and P. Huang, *Chem. Soc. Rev.*, 2018, **47**, 6454–6472.
128 C. Wei, Y. Liu, X. Zhu, X. Chen, Y. Zhou, G. Yuan, Y. Gong and J. Liu, *Biomaterials*, 2020, **238**, 119848.
129 X. Wan, L. Song, W. Pan, H. Zhong, N. Li and B. Tang, *ACS Nano*, 2020, **14**, 11017–11028.
130 Y. Ouyang, P. Wang, B. Huang, G. Yang, J. Tian and W. Zhang, *ACS Appl. Bio Mater.*, 2021, **4**, 4413–4421.
131 Y. Xue, J. Tian, Z. Liu, J. Chen, M. Wu, Y. Shen and W. Zhang, *Biomacromolecules*, 2019, **20**, 2796–2808.
132 J. Mendelsohn, *Clin. Cancer Res.*, 1997, **3**, 2703–2707.
133 H. He, Y. Chen, Y. Li, Z. Song, Y. Zhong, R. Zhu, J. Cheng and L. Yin, *Adv. Funct. Mater.*, 2018, **28**, 1706710.
134 L. Ding, X. Lin, Z. Lin, Y. Wu, X. Liu, J. Liu, M. Wu, X. Zhang and Y. Zeng, *ACS Appl. Mater. Interfaces*, 2020, **12**, 36906–36916.
135 K. Sinha, J. Das, P. B. Pal and P. C. Sil, *Arch. Toxicol.*, 2013, **87**, 1157–1180.
136 C. Roma-Rodrigues, L. Rivas-García, P. V. Baptista and A. R. Fernandes, *Pharmaceutics*, 2020, **12**, 233.
137 P. R. Cullis and M. J. Hope, *Mol. Ther.*, 2017, **25**, 1467–1475.
138 H. Wang, Y. Chen, H. Wang, X. Liu, X. Zhou and F. Wang, *Angew. Chem., Int. Ed.*, 2019, **58**, 7380–7384.
139 D. A. Baum and S. K. Silverman, *Cell. Mol. Life Sci.*, 2008, **65**, 2156–2174.
140 H. Fan, X. Zhang and Y. Lu, *Sci. China: Chem.*, 2017, **60**, 591–601.
141 A. J. Amali, H. Hoshino, C. Wu, M. Ando and Q. Xu, *Chemistry*, 2014, **20**, 8279–8282.
142 D. Wang, D. Jana and Y. Zhao, *Acc. Chem. Res.*, 2020, **53**, 1389–1400.
143 C. Sui, R. Tan, Y. Chen, G. Yin, Z. Wang, W. Xu and X. Li, *Bioconjugate Chem.*, 2021, **32**, 318–327.
144 S. Wang, L. Shang, L. Li, Y. Yu, C. Chi, K. Wang, J. Zhang, R. Shi, H. Shen, G. I. Waterhouse, S. Liu, J. Tian, T. Zhang and H. Liu, *Adv. Mater.*, 2016, **28**, 8379–8387.
145 Q. Zhang, J. He, W. Yu, Y. Li, Z. Liu, B. Zhou and Y. Liu, *RSC Med. Chem.*, 2020, **11**, 427–437.
146 L. Zhang, Z. Yang, W. He, J. Ren and C.-Y. Wong, *J. Colloid Interface Sci.*, 2021, **599**, 543–555.
147 B. Wu, J. Fu, Y. Zhou, S. Luo, Y. Zhao, G. Quan, X. Pan and C. Wu, *Acta Pharm. Sin. B*, 2020, **10**, 2198–2211.
148 M. Ma, A. Bétard, I. Weber, N. S. Al-Hokbany, R. A. Fischer and N. Metzler-Nolte, *Cryst. Growth Des.*, 2013, **13**, 2286–2291.
149 C. Mellot-Draznieks, C. Serre, S. Surblé, N. Audebrand and G. Férey, *J. Am. Chem. Soc.*, 2005, **127**, 16273–16278.
150 X. Sun, G. He, C. Xiong, C. Wang, X. Lian, L. Hu, Z. Li, S. J. Dalgarno, Y.-W. Yang and J. Tian, *ACS Appl. Mater. Interfaces*, 2021, **13**, 3679–3693.
151 J.-C. Yang, Y. Shang, Y.-H. Li, Y. Cui and X.-B. Yin, *Chem. Sci.*, 2018, **9**, 7210–7217.
152 G. K. Gupta and D. K. Agrawal, *BioDrugs*, 2010, **24**, 225–235.
153 G. Turgeon, A. Weickhardt, A. Azad, B. Solomon and S. Siva, *Med. J. Aust.*, 2019, **210**, 47–53.
154 W.-D. Yu, G. Sun, J. Li, J. Xu and X. Wang, *Cancer Lett.*, 2019, **452**, 66–70.
155 R. Xie, P. Yang, S. Peng, Y. Cao, X. Yao, S. Guo and W. Yang, *J. Mater. Chem. B*, 2020, **8**, 6128–6138.
156 M. P. Cuajungco, M. S. Ramirez and M. E. Tolmasky, *Biomedicines*, 2021, **9**, 208.
157 P. Chen, M. He, B. Chen and B. Hu, *Ecotoxicol. Environ. Saf.*, 2020, **205**, 111110.